PLASMA WAVES ASSOCIATED WITH THE SPACE SHUTTLE

I.H. Cairns & D.A. Gurnett

Department of Physics & Astronomy, University of Iowa, Iowa City, USA

ABSTRACT

Water molecules outgassed from the US/NASA space shuttle suffer collisional charge-exchange with ionospheric oxygen ions, thereby forming unstable distributions of pick-up water ions and leading to high levels of plasma waves near the shuttle. Liouville's equation with a charge-exchange source term is solved for the water ion distribution function as a function of position relative to the shuttle. The observational characteristics of the near zone shuttle waves are summarized. A linear theory in which beam-like distributions of water ions drive Doppler-shifted lower hybrid waves via the modified-two-stream instability is developed. This theory explains many characteristics of the near zone waves. However, further work on the effects of wave nonlinearities and spatial inhomogeneity is required to explain the detailed frequency spectrum of the waves. The observed wave levels apparently satisfy the threshold condition for modulational instability of lower hybrid waves.

Key words: Waves; Instabilities; Pick-up ions; Lower hybrid; Space shuttle.

1. INTRODUCTION

This paper discusses the water ions and high levels of plasma waves found in the immediate vicinity of the USA/NASA space shuttle. At first sight then, the presentation of this paper at a conference on Plasma Astrophysics might appear rather unusual. Three justifications for including this paper are: (1) Water ion pick-up phenomena strongly influence the plasma and wave environment of the shuttle, very similar to the case of comets in our solar system (e.g., Ref. 1 and references therein). (2) The paper addresses issues in basic plasma physics and space plasma physics such as the modified-two-stream instability and possible strong turbulence collapse of lower hybrid waves (e.g., Ref. 2 and references therein). (3) The increasing importance of space-based instruments in astrophysics requires that any perturbations to the local plasma caused by the orbiting platform be understood. More complete descriptions of the work presented here will be available shortly (Refs. 3-5).

The gaseous and plasma environment of the space shuttle and the interaction of the shuttle's atmosphere with the ionospheric plasma has been investigated by the OSS-1 and Spacelab-2 shuttle missions. These and other missions found the shuttle environment to be surprisingly active, as reviewed by Shawhan et al. (Ref. 6) and Kurth and Frank (Ref. 7), with high levels of several types of plasma waves (Refs. 4, 5, 8, 9), energetic pick-up ions and other particles (Ref. 10), multiple ion streams (Ref. 11), and many ionic species such as H_2O^+ and H_3O^+ (references in Ref. 10). Measurements of these phenomena were performed with instruments mounted on a pallet within the shuttle's payload bay and exposed to space, and on a small independent spacecraft, the Plasma Diagnostics Package or PDP (Refs. 12 and 7). This PDP spacecraft probed the shuttle's environment both while attached to the shuttle and while flying free of the shuttle (the so-called "free-flight" mission) to distances of order 400 m.

The general scenario envisaged (e.g., Refs. 6,9,10) for the shuttle's interaction with the ionospheric plasma involves the outgassing of water vapour from the shuttle orbiter, the subsequent collisional charge-exchange of these water molecules with ionospheric oxygen ions (O^+) to form water ions, the generation of plasma waves by these water ions, and subsequent plasma heating and the production of energetic particles. Evidence exists for a cloud of neutral water vapour surrounding the shuttle (Refs. 13-15), and water ions have indeed been observed, both by the shuttle's payload instruments (Refs. 14,15) and by the PDP instruments (Ref. 10). During the PDP's free-flight around the space shuttle (Spacelab-2), Paterson and Frank (Ref. 10) observed "ring-like" distributions of ions with the basic characteristics expected of water ions produced by the charge-exchange process. They also found that the observed number densities of the ring-like distributions were qualitatively and often quantitatively consistent with those predicted by a theoretical model for production of water ions by charge-exchange from a water cloud surrounding the space shuttle out to distances of at least 400 m.

This paper presents an overview of progress on 3 problems corresponding to plasma waves associated with the space shuttle. In Section 2 we construct a theory for the water ion distribution function close to the space shuttle using solutions to Liouville's equation with a charge-exchange source term; in particular we show that the distribution function smoothly varies from a ring-like distribution to a beam-like distribution with distance from the space shuttle. The spatial variation in the number density of water ions is also addressed. In Section 3 we present observational data on the characteristics of the near zone (within 10 m) shuttle waves and summarize data presented in Ref. 5. In Section 4 we present a linear theory for the observed waves in terms of Doppler-shifted lower hybrid waves driven by beam-like water ions via the modified-two-stream instability. This linear theory predicts wave characteristics consistent with the characteristics of the observed waves except for the detailed form of the frequency spectrum. The effects of spatial inhomogeneity and nonlinearities due to the high wave levels present are appealed to as the cause of the observed wave frequency spectrum. Brief conclusions to the paper are provided in Section 5.

2. THE DISTRIBUTION FUNCTION OF WATER IONS

Knowledge of the particle distribution functions and sources of free energy is a prerequisite for constructing

Proceedings of the joint Varenna-Abastumani-ESA-Nagoya-Potsdam Workshop on 'Plasma Astrophysics' held in Telavi, Georgia, USSR, 4–12 June 199((ESA SP-311, August 1990).

theories for the active and complex wave environment in the near vicinity of the space shuttle. However, at the present time published observational data on the distribution functions of the pick-up water ions within 50 m of the shuttle do not exist. Accordingly, the problems of the water ion distribution function and the source of free energy driving the observed waves in the very near vicinity of the space shuttle must be attacked theoretically. We note that Paterson and Frank's (Ref. 10) previous theoretical analysis ignored the particle distribution function in favour of a fluid description and did not consider the effects of the large water ion gyroradius (~ 40 m).

2.1 Physical Model

We consider a reference frame (X_p, Y_p, Z_p) moving with and centered on the space shuttle in which the ionospheric magnetic field $\underline{B}_0$ is along the Z_p axis. The velocity of the background plasma in this reference frame is generally of the form ($-V_\perp$, 0, $-V_\parallel$); positive values of X_p then correspond to the region upstream of the shuttle. The motion of the background plasma across the magnetic field implies the presence of a self-consistent electric field $\underline{E}$=(0, $-V_\perp B_0$, 0) in this reference frame. Velocity is conserved during the charge-exchange process. Now, however, the newly-born water ion must respond to the crossed electric and magnetic fields, resulting in a cycloidal motion in the X_p-Y_p plane. The equations of motion for the particle motion may be solved for the position and velocity of the particle as a function of time given the position and velocity at some reference time. This motion may be summarized as follows: firstly, any particle speed along the magnetic field (the Z_p axis) remains constant; secondly, ignoring thermal motions for the moment, a newly-born water ion starts out at zero velocity and is accelerated by the crossed electric and magnetic fields into motions with a gyrospeed $V_\perp$ centered on a velocity ($-V_\perp$, 0, 0). This gyromotion maps out a ring in the X_p-Y_p plane. A "ring" distribution results if water ions are found at all gyrophases in this X_p-Y_p plane, while a "beam" distribution results if the water ions are found in a well-defined range of gyrophases. Thermal motions produce a spread in gyrospeed and velocity along the magnetic field. Fig. 1 illustrates a partial ring distribution, which will be called a beam arc distribution below.

Liouville's equation for the distribution function of charge-exchanged water ions, $f_w(\underline{r}, \underline{p}, t)$, is

$$\frac{d}{dt} f_w(\underline{r}, \underline{p}, t) = F_w(\underline{r}, \underline{p}, t) \qquad (1)$$

where $F_w(\underline{r}, \underline{p}, t)$ is the source term. A formal solution exists:

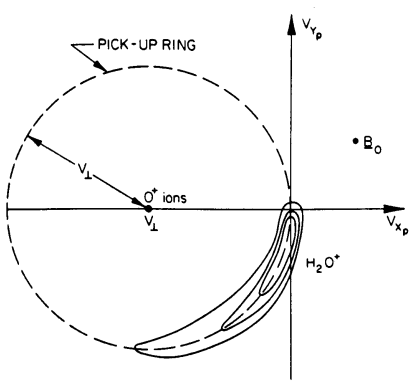

Fig. 1. Beam arc distribution displayed in V_{X_p}-V_{Y_p} space. Water ions are created near zero velocity and follow their gyromotion clockwise around the dashed 'pick-up' ring.

$$f_w(\underline{r}, \underline{p}, t) = \int_{-t}^{0} d\tau F_w(\underline{r}'(\underline{r}, \underline{p}, t; \tau), \underline{p}'(\underline{r}, \underline{p}, t; \tau), t + \tau) \qquad (2)$$

where $\underline{r}'(\underline{r}, \underline{p}, t; 0) = \underline{r}$, $\underline{p}'(\underline{r}, \underline{p}, t; 0) = \underline{p}$, and τ is the travel time from ($\underline{r}'$, $\underline{p}'$) to ($\underline{r}$, $\underline{p}$) along the particle path. The effects of wave-particle scattering on the particle distribution function are ignored in this treatment.

An expression for the source term $F_w(\underline{r}, \underline{p}, t+\tau)$ for the collisional charge-exchange follows from the binary nature of the collision and conservation of velocity for the particles:

$$F_w(\underline{r}, \underline{p}, t + \tau) = \gamma n_{O+}(\underline{r}, t + \tau) f_m(\underline{r}, \underline{p}, t + \tau) \qquad (3)$$

where n_{O+} is the number density of oxygen ions. This equation is consistent with the usual charge-exchange equation involving number densities, allowing identification of the reaction rate γ as 2 x 10^{-9}cm^{3}s^{-1} (Ref. 10). The remaining quantity f_m is the distribution function of the water gas molecules, which for time-steady outflow with thermal speed V_m from the shuttle may be written as the product of the oxygen ion number density, which varies inversely with radial distance squared, and a Maxwellian velocity distribution with isotropic thermal speed V_m. For convenience we now assume that the velocity and density of the background plasma, the magnetic field strength, and water gas thermal speed are constant over the timescales of interest. Normalizing all speeds by the water thermal speed V_m and distances by the characteristic distance V_m/f_{gw} (f_{gw} is the gyrofrequency of a water ion) these assumptions and Eq. 3 allow Eq. 2 to be rewritten as the product of constants times a "probability" integral for the charge-exchange:

$$f_w(\underline{r}, \underline{p}, t) = \frac{\gamma n_{O+} n_0 r_0^2}{(2\pi)^{3/2}} \int_{-t}^{0} d\tau \frac{e^{-v'^2(\underline{r}, \underline{p}, t+\tau)/2}}{r'^2(\underline{r}, \underline{p}, t + \tau)} \qquad (4)$$

with r' and v' implied by Eqs. 3 and 4 and the equations of motion for the water ions. Here $n_0(r_0)$ is the number density of water molecules at a radial distance r_0 from the shuttle and the symbol v denotes the speed corresponding to momentum $\underline{p}$. The "probability" integral, essentially an integral over travel time $|\tau|$ of the probability of charge-exchange producing ions at earlier times $t+\tau$ with eventual momentum $\underline{p}$ at the observation time t and position $\underline{r}$, may be performed numerically using standard techniques. The shape of the distribution function is specified by the probability integral alone. Before proceeding we specify the nominal parameters used in the calculations below. Assuming a constant water gas temperature of 300K, a typical (normalized) value of $V_\perp$ is 20 and the distance scale V_m/f_{gw} is 15 m.

2.2 Distribution Functions Directly Upstream from the Shuttle

Fig. 2 shows the water ion distribution functions resulting from charge-exchange at two distances directly upstream from the shuttle (Y_p=Z_p=0) and demonstrates the transition from a ring distribution to a beam-like distribution with decreasing distance from the shuttle. These distributions are displayed as contour plots in a gyrospeed-gyrophase phase space formed by unfolding the ring feature in X_p-Y_p velocity space (e.g., Fig. 1) centered on the velocity ($-V_\perp$, 0, 0) for particles with zero speed along the magnetic field. For reference, an ion formed by pick-up of a water molecule with zero initial velocity in the shuttle frame has gyrospeed $V_\perp$, initially has zero gyrophase, and has a gyrophase which increases with time as the ion follows its gyromotion. A ring distribution then has contours which do not vary greatly with gyrophase, as is the case at the position X_p=50, far upstream from the shuttle orbiter, shown in Fig. 2(a). A beam distribution has contours which delineate a limited range of gyrophases; Fig. 2(b) shows that the distribution at X_p=2 (close to the shuttle) has some beam-

like characteristics at small gyrophases. In these figures the contours are logarithmically spaced (to the base 10) in arbitrary units. We note that the significant velocity spread of the distribution even at X_p=1 implies that it is therefore not appropriate to term these water ion distributions "beam" distributions in an absolute sense. Rather, we suggest the term "beam arc" distributions, corresponding to a finite segment of a ring, to describe these ion distributions found close to the shuttle. We note, however, that these beam arc distributions do have some beam-like characteristics so that instability calculations assuming conventional beams may provide a reasonable first description of an instability.

This transition from ring to beam arc distribution function with position upstream from the shuttle may be understood in terms of the spatial gradient in water molecule number density and the characteristics of the charge-exchange process. Fig. 3 illustrates the development of beam arc and ring distributions at X_p=1 and X_p=15, respectively, in the X_p-Y_p plane for $V_\perp$=20. The solid lines are contours of constant inverse distance squared $1/R_p^2$, and so constant charge-exchange rate, spaced in powers of 10. The characteristics of the water ion distribution function at X_p=1 and X_p=15 follow on considering the primary sources of particles with zero velocity (stars) and velocity ($-2V_\perp$, 0, 0) (boxes) at the observation points. Ignoring thermal motions (i.e., $V_m \ll V_\perp$), all pick-up water ions initially have zero velocity. Particles observed at zero velocity are therefore primarily produced (at the star symbols) very close to the observation point. Particles observed at velocity ($-2V_\perp$, 0, 0) have, however, followed their gyromotion along the dashed lines from their primary production points (boxes) where they had zero velocity. At X_p=1, therefore, the production rate of water ions observed at velocity ($-2V_\perp$, 0, 0) is less than one hundredth that for ions observed near zero velocity, implying that the distribution function is a well-defined beam arc. In contrast, at X_p=15 the production rates for ions with near-zero velocity and velocity ($-2V_\perp$, 0, 0) differ by only a factor $(15/25)^2 \sim 0.4$, implying a ring distribution function with small contrast as in Fig. 2a. Farther from the shuttle the ring distributions become more uniform. Beam arcs do not form exactly at zero gyrophase due to the thermal spread of the water molecules.

Beam arc water distributions are also formed away from the X_p axis in the upstream region in regions where the charge-exchange rate is large. A general condition for formation of a beam arc distribution is that R_p<2 with X_p>0. In summary, the water ions should have a beam arc distribution function when upstream and within a radial distance of order 20-40 m (R_p<2) from the shuttle in the upstream hemisphere.

2.3 Discussion

The above results show that beam arc distributions of water ions, with considerable gyrophase anisotropies, should exist at positions close to and upstream from the space shuttle. In contrast, Paterson and Frank [1989], and Paterson [1987], do not report observations of gyrophase anisotropies for their pick-up ions. This is not inconsistent with the work described in this paper due to (1) the PDP spacecraft's orbit around the shuttle not sampling the required region where such anisotropies are significant, and (2) the beam arc distributions being near zero velocity in the upstream region and so being removed from Paterson and Frank's analysis due to potential confusion with ambient oxygen plasma. Furthermore, elsewhere we will show that the water ion distribution functions predicted by our Liouville calculation are primarily ring-like (with no well-defined beam arcs) for the entire duration of the PDP's free-flight motion around the space shuttle during the Spacelab-2 mission.

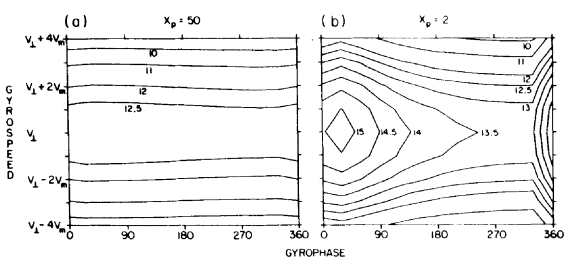

Fig. 2. Contour plots of the water ion distribution function in a gyrospeed-gyrophase phase space at two positions along the X_p axis. Contours are logarithmic to the base 10. (a) A ring distribution at X_p=50. (b) A beam arc distribution of X_p=2.

The water ion distribution functions derived using the Liouville code may be integrated numerically to give the water ion number density as a function of position relative to the space shuttle (Ref. 3). This work may be summarized as follows: (1) Relative water ion (to plasma) densities should exceed 1% within approximately 150 m of the shuttle. (2) Within 10 m of the shuttle water ions should comprise at least 20% of the plasma density. (3) Pile-up of water ions due to kinematic effects leads to an increase in plasma density close to the shuttle. This pile-up is not included in fluid predictions for the water ion number density. We note that water ions and other pick-up ions sometimes comprise at least 50% of the plasma density in the near vicinity of the space shuttle (e.g., Ref. 7). Accordingly, non-Maxwellian distributions of water ions with significant densities should be strongly considered when interpreting the data from the OSS-1 and Spacelab-2, and perhaps other, shuttle missions.

Lastly, elastic and charge-exchange collisions between the water ions and water gas molecules offer another means of establishing more beam-like water ion distribution functions: the beam arc distributions occur due to the water ions following their gyromotion; disruption of the regular ion gyromotion by collisions with low velocity water neutrals might then limit the water ions to a more limited range of gyrophases and so to a more beam-like distribution function. Further work is required to see whether such collisions are important in determining the water ion distribution function close to the shuttle.

3. CHARACTERISTICS OF THE NEAR ZONE SHUTTLE WAVES

One of the unexpected results from the OSS-1 mission was the observation of high levels of broadband electrostatic

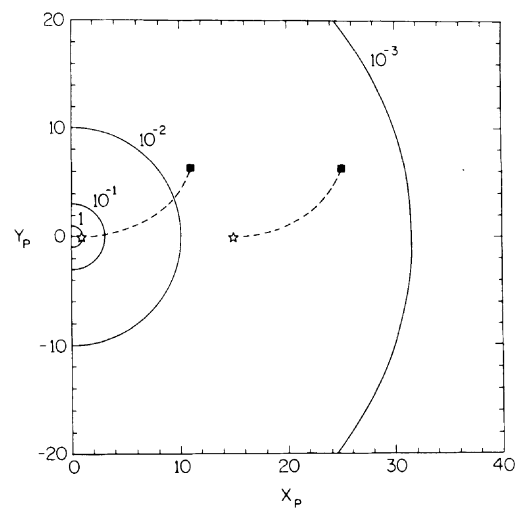

Fig. 3. Formation of beam arc and ring distributions close to and far from the space shuttle, respectively. See text for explanation.

waves in the very near vicinity (within 10 meters) of the space shuttle (Refs. 6,8). The waves had their greatest spectral densities between 31 Hz (the lowest frequency measured) and about 31 KHz, with a peak between 100 Hz and 300 Hz, but extended in frequency above 100 KHz. In comparison, during this mission, the ion gyrofrequency was of order 50 Hz, the lower hybrid frequency was of order 5 KHz, and the oxygen ion plasma frequency was of order 15-55 KHz. Here we summarize observational data from the XPOP roll during the Spacelab-2 mission, presented in detail in Ref. 5, which characterize the waves in sufficient detail for theoretical progress to be made.

Fig. 4 shows the time-averaged spectral density of the near zone waves as a function of frequency. This figure clearly shows a fall-off at low frequencies, the presence of a low frequency peak near 178 kHz, a region with spectral densities decreasing approximately inversely with frequency between the low frequency peak and the lower hybrid frequency, a bulge around the lower hybrid frequency, and a rapid fall-off at higher frequencies. One implication of these data is that the electric field in the waves should be approximately constant between 100 Hz and the lower hybrid frequency, and essentially negligible at higher frequencies.

Fig. 5 shows the relative contribution of the electric fields centered on the i'th channel to the total average broadband, frequency-integrated electric field E_T plotted versus the frequency of the i'th channel. The detailed definition of this quantity is $R(f_i) = E_i/\Sigma_i E_i$ with $E_i^2 = \int S(f)df$ with upper and lower limits of integration $f_U = \sqrt{f_i f_{i+1}}$ and $f_L = \sqrt{f_i f_{i-1}}$, respectively. Here S(f) is the spectral density, and the frequency intervals for integration are equally spaced in logarithmic frequency. The data plotted are for the period 0145-0210 shown in Fig. 4. The total average broadband electric field E_T was 51.1 mV/m. As anticipated above, the electric field is essentially constant between 100 Hz and the lower hybrid frequency, and essentially negligible at higher frequencies. Two peaks, a factor of order 2 above the uniform level, are visible. The first is at low frequencies centered on 178 Hz, with a broad shoulder at significant amplitudes to the second peak which is situated between 5.6 KHz and 10 KHz. As described above, the lower hybrid frequency varies between 5 and 10 KHz during this time period, providing an excellent identification for the higher frequency peak. Above 56 KHz the measured electric fields are essentially negligible. Murphy et al. (Ref. 8) and Shawhan et al. (Ref. 6) have previously recognized the existence of the low frequency peak. However, neither the essentially constant level of waves between the 100 Hz and the lower hybrid frequency, nor the peak near the lower hybrid frequency have been recognized before.

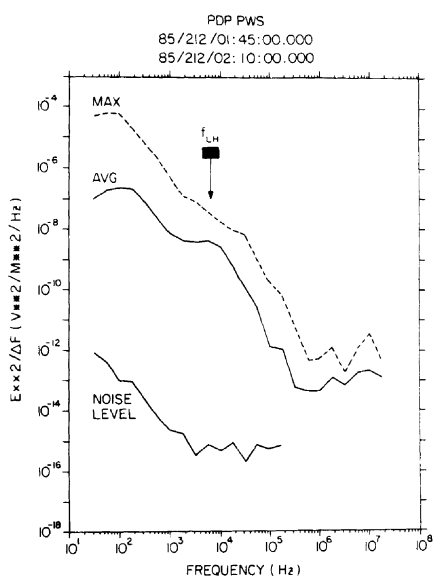

Fig. 4. Spectral density as a function of frequency for the period 01:450-2:10, day 212, 1985, during the XPOP roll.

The interpretation of these data in terms of components in the wave spectrum is not unique. However, it seems most appropriate to interpret the wave spectrum in terms of a fairly constant high level of waves (electric fields of order 2.5 mV/m per frequency interval) from 31 Hz to 10 KHz with two superposed peaks, one around 178 Hz and one near the lower hybrid frequency. These superposed peaks have electric fields a factor of two higher than the constant level of waves between 30 Hz and 10 KHz. These data require any high frequency waves above about 20 KHz to smoothly merge with the lower hybrid frequency waves; no evidence is found for any sharply peaked wave components in the frequency range of 10 to 40 KHz. These identifications are referred to below as the 'uniform' component, the low frequency component and the lower hybrid component. A theoretical interpretation for the uniform component is developed in the next section, while suggestions for the two peak components are given in Ref. 5.

The other results reported in Ref. 5 are as follows.

- Null features in the wave data as the PDP spacecraft moves through the shuttle's plasma wake imply that the higher frequency near zone waves have smaller wavelengths (higher wavenumbers).
- Observations of the near zone waves while the PDP was magnetically connected to the space shuttle at a distance of order 200 m imply that the near zone waves have wavevectors perpendicular to the magnetic field.
- The near zone waves show a pronounced decrease in amplitude and spectral extent when the shuttle is moving most nearly parallel to the magnetic field. This so-called $V_\parallel/V_T$ effect implies that the near zone waves are driven by water pick-up ions.

4. A NEW THEORY FOR THE NEAR ZONE WAVES: DOPPLER-SHIFTED LOWER HYBRID WAVES

Two previous theories for the near zone shuttle waves are discussed in detail in Ref. 5. Hwang et al. (Ref. 16) proposed that the waves result from ion acoustic or ion-ion acoustic instabilities driven by the secondary ion streams observed (Ref. 11) in the near vicinity of the space shuttle. This theory is inconsistent with the frequency spectrum and wavevector directions of the near zone waves reported in Ref. 5. Papadopoulos (Ref. 17) proposed that the waves are Doppler-shifted lower hybrid waves driven via the modified-two-stream instability by ionospheric oxygen ions reflected from the shuttle. This theory fails on two grounds. Firstly, severe theoretical problems exist for

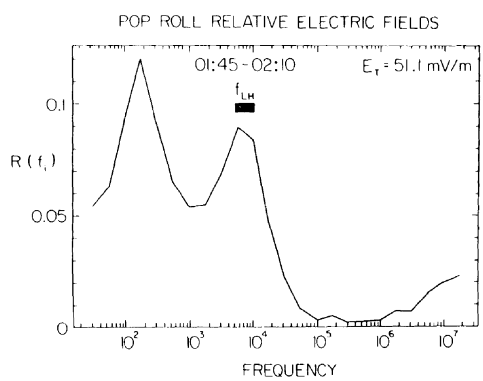

Fig. 5. Radio R(f) of the average electric field in a frequency bandwidth divided by the total average broadband field as a function of frequency (see text for a detailed definition).

reflections of charged oxygen ions at significant yields (>1%) at these low collision energies (5 eV). Secondly, correcting a minor error in Papadopoulos' calculation of the observed wave frequencies leads to the prediction that the waves should have frequencies in the range from 0.5-1.4 f_{LH}, thereby not explaining the large wave levels below 1 KHz. In addition, no simple explanation of the observed $V_\parallel/V_T$ effect is apparent for these theories.

Here we propose a new theory: the waves are Doppler-shifted lower hybrid waves driven via the modified-two-stream instability by beam arc distributions of water ions in the near vicinity of the space shuttle. These water ions naturally comprise at least 20% of the plasma densities, thereby greatly favouring this theory over Papadopoulos' theory. In addition, a natural explanation for the $V_\parallel/V_T$ effect is available. In this first development of the theory we represent the water ions as a Maxwellian beam distribution centered at zero velocity while the ionospheric electrons and oxygen ions have Maxwellian distributions drifting relative to the water ions. We restrict ourselves to the case in which the shuttle moves exactly perpendicular to the magnetic field ($V_\parallel$=0). Making the standard approximations (e.g., Ref. 17) we can reduce the exact electrostatic dispersion equation ($\beta<10^{-5}$) to the standard form for the modified-two-stream instability:

$$1 - \frac{n_O}{n_e}\frac{\Omega_{LH}^2}{(\omega - k_x V_\perp)^2} - \frac{n_w}{n_e}\frac{\Omega_{LH}^2}{\omega^2} = 0. \qquad (5)$$

Here, the quantity $\omega - k_x V_\perp$ is the Doppler-shifted wave frequency seen by the ionospheric electrons and oxygen ions. Subscripts e, O, and w refer to the electrons, oxygen ions and water ions, respectively. A positive component k_x for a wavevector implies the wavevector is directed upstream along the X_p axis. This equation is directly analogous to the dispersion equation for the usual two-stream instability in which Langmuir waves are generated by an electron beam and viewed in the reference frame of the beam (Ref. 18). Accordingly, for water ion beams which satisfy the condition $n_w/n_e > 2.5(V_w/V_\perp)^3$ ($\sim 10^{-3}$ here), this equation predicts generation of strongly growing waves with dispersion relation $\omega_{rest} \sim k_x V_\perp$, wavevectors approximately perpendicular to the magnetic field, frequencies near the lower hybrid frequency in the ionospheric plasma rest frame, and relatively small wave frequencies in the shuttle's rest frame.

Fig. 6 shows the wave dispersion relation and growth rate in the ionospheric plasma frame obtained by solving the full electrostatic dispersion equation numerically (including electron and oxygen ion magnetization) for waves propagating along the X_p direction with an angle θ=89.9° between the wavevector and the magnetic field direction (the Z_p axis). The dashed line shows the dispersion relation $\omega_{rest} = k_x V_\perp$ for comparison. A strong resemblance to the ordinary beam instability for "Langmuir" waves is apparent (e.g., Fig. 1 of Ref. 18). Four important results may be inferred from this figure: (1) These waves are essentially beam driven waves with $\omega_{rest} \sim k_x V_\perp$. (2) The waves have strong growth rates. (3) Noting that $\omega_r < k_x V_\perp$ for all wavenumbers k_x, these waves will be Doppler-shifted to low and negative frequencies (only the magnitude of the frequency is directly observable, however). (4) The higher wavenumber waves will be Doppler-shifted to larger observable wave frequencies than the smaller wavenumber waves.

Further calculations show that the growing waves are severely restricted in angle θ, as expected for lower hybrid waves. Fig. 7 shows plots of observable wave frequency versus growth rate for various ratios of water ion to electron number density at the angles θ of maximum growth rate. The theory predicts waves in the observed frequency range. Increasing the water ion number density increases both the center frequency and bandwidth of the growing waves. Accordingly, linear theory predicts that the spatial gradient in water ion number density near the shuttle (Ref. 3), when not in the wake region, implies an increase in the center frequency, bandwidth and growth rate of the unstable waves with decreasing distance from the shuttle. The linear theory can therefore explain wave growth from near zero frequency up to a frequency of order f_{LH} as required.

In summary, this linear theory is capable of explaining the generation of waves (1) with large growth rates in the observed frequency range and range of observable wavenumbers, (2) with wavevectors essentially perpendicular to the magnetic field, (3) with wavenumber increasing with frequency. The theory also admits natural explanations for the observed $V_\parallel/V_T$ effect. Unusual species temperatures, densities, or preheating of the electrons are not required. However, the linear theory is not capable of explaining the details of the frequency spectrum for the intense near zone waves. In particular the linear theory predicts peak growth in the range 0.25-0.75 f_{LH} (depending on the relative number density of water ions as in Fig. 7), well above the

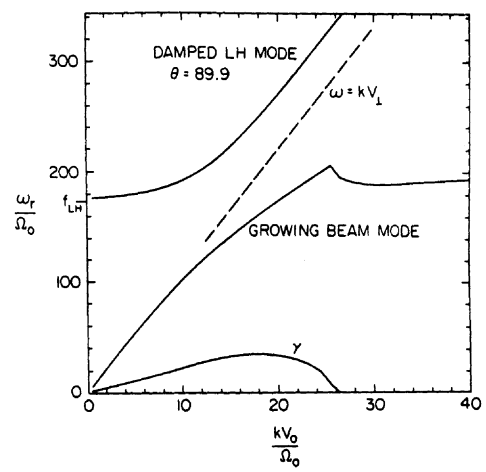

Fig. 6. Dispersion diagram (in the ionospheric plasma frame) for waves driven by a water ion beam with n_w/n_e= 0.05 and wavevectors defined by θ=89.9°. The damped lower hybrid mode and growing beam mode waves are shown. Subtraction of $kV_\perp$ gives the wave frequency in the observing frame.

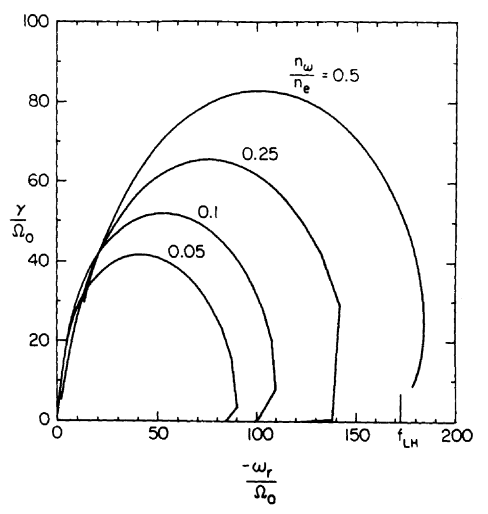

Fig. 7. Growth rates versus (observable) wave frequency as a function of beam density n_w/n_e for angles θ with the maximum growth rate and wavevectors in the X_p-Z_p plane.

observed low frequency peak at about 178 Hz and well below the observed peak near the lower hybrid frequency. This difficulty in explaining the details of the observed frequency spectrum should be expected for at least three reasons. Firstly, the preliminary nature of this linear theory, secondly the neglect of inhomogeneity effects in the strongly inhomogeneous shuttle environment, and thirdly the neglect of nonlinear effects which are often vital in determining the wave spectrum. Further discussion of improvements to the linear theory and the role of inhomogeneity effects is given in Ref. 5. Only nonlinear effects are briefly and qualitatively discussed here.

Nonlinear processes involving lower hybrid waves, such as scattering off thermal ions, decay processes involving ion acoustic waves, modulational instabilities and strong turbulence processes, have been discussed in the literature (e.g., Ref. 2, 19). Detailed discussions of these possibilities are not appropriate here. Here we note that the ratio of wave electric field energy to thermal plasma energy is of order 10^{-5} (for $n_e=10^{11}m^{-3}$) while the ratio of the total water ion kinetic energy to the thermal plasma energy is of order 5 for $n_w/n_e=0.1$. Moreover, the wavelengths predicted by the linear theory are smaller than (but comparable to) the PDP's effective antenna length during the XPOP roll (1.15 m), indicating that the wave levels in the plasma may be underestimated. These wave levels are considerable and imply that nonlinear processes, including strong turbulence processes, warrant considerable attention. In particular, the equations in Ref. 2 suggest that the threshold for the modulational instability is at least marginally satisfied for these waves. Further support for consideration of nonlinear effects comes on comparing the timescales for growth and convection of the waves. For waves with a linear growth rate of $50\Omega_O$ typical in Fig. 15, 10 e-folding periods corresponds to a time of 10^{-3} seconds. During this time period a wave packet would be convected a maximum distance of 8 m (given the shuttle's orbital speed of 7.8 Kms^{-1}) while a wave's electric field would increase by a factor of 2×10^4. This distance is small compared with the expected extent of the region near the shuttle with beam distributions of water ions (~ 30m).

5. CONCLUSIONS

This paper shows that ion pick-up phenomena control the plasma wave environment of the USA/NASA space shuttle, similar to the situation at comets. We have developed a theory for the water ion distribution function resulting from charge-exchange of outgassed water molecules. This theory, involving the solution of Liouville's equation with a charge-exchange source term, predicts a transition from ring-like distributions to beam arc distributions with decreasing distance upstream from the shuttle. The characteristics of the observed near zone (within 10 m of the shuttle) waves are summarized. A linear theory involving Doppler-shifted lower hybrid waves driven by beam arc distributions of water ions via the modified-two-stream instability is developed. This theory can explain most characteristics of the observed waves. However, appeals to the effects of wave nonlinearities and spatial inhomogeneity are required to explain the details of the observed frequency spectrum. Further work on these matters is required. The high wave levels present apparently exceed the threshold condition for modulational instability of lower hybrid waves, thereby providing some support for nonlinear effects being important.

6. ACKNOWLEDGEMENTS

The authors thank J.S. Pickett, W.S. Kurth, C.K. Goertz, W.R. Paterson, N. D'Angelo, and L.A. Frank for helpful discussions concerning the PDP data and the shuttle's plasma environment. Financial support from NASA Grants NAGW-1488 and NAG3-449 from NASA Headquarters and NASA/Lewis Research Center, respectfully, is gratefully acknowledged.

7. REFERENCES

1. Johnstone AD et al. 1990, Observations in the bow shock of comet Halley, this issue.
2. Kalinin VP et al. 1990, Lower hybrid collapse dynamics in the space plasma, this issue.
3. Cairns IH 1990, Transition from ring to beam arc distributions of water ions near the space shuttle orbiter, *J. Geophys. Res.*, in press.
4. Cairns IH and Gurnett DA 1990, Control of plasma waves associated with the space shuttle by the angle between the orbiter's velocity vector and the magnetic field, *J. Geophys. Res.*, submitted.
5. Cairns IH and Gurnett DA 1990, Plasma waves observed in the near vicinity of the space shuttle, *J. Geophys. Res.*, submitted.
6. Shawhan SD et al. 1984, Plasma Diagnostics Package initial assessment of the shuttle orbiter plasma environment, *J. Spacecraft Rockets*, **21**, 387-391.
7. Kurth WS and Frank LA 1990, The Spacelab-2 Plasma Diagnostics Package, *J. Spacecraft Rockets*, **27**, 70-75.
8. Murphy GB et al. 1983, Interaction of the space shuttle orbiter with the ionospheric plasma, *Spacecraft/Plasma Interactions and Their Influence on Field and Particle Measurement*, ESA SP-198, 73.
9. Gurnett DA et al. 1988, Plasma wave turbulence around the shuttle: Results from the Spacelab-2 flight, *Geophys. Res. Lett.*, **15**, 760-763.
10. Paterson, WR and Frank LA 1989, Hot ion plasmas from the cloud of neutral gases surrounding the space shuttle, *J. Geophys. Res.*, **94**, 3721-3727.
11. Stone NH et al. 1983, Multiple ion streams in the near vicinity of the space shuttle, *J. Geophys. Res.*, **10**, 1215-1218.
12. Shawhan SD 1982, Description of the Plasma Diagnostics Package (PDP) for the OSS-1 shuttle mission and JSC chamber test in conjunction with the fast pulse electron gun (FPEG), *Artificial Particle Beams in Space Plasma Studies*, ed. B. Grandel, Plenum, New York, 419-430.
13. Carignan GR and Miller ER 1983, Mass spectrometer STS-2, -3, -4 induced environment contamination monitor (IECM) summary report, ed. ER Miller, *NASA Tech. Memo.*, NASA TM-82524, 87-101.
14. Narcisi R et al. 1983, The gaseous and plasma environment around space shuttle, *AIAA Pap.*, 83-2659.
15. Koch DG et al. 1987, Infrared observations of contaminants from shuttle flight 51-F, *Adv. Space Res.*, **7**, 211-221.
16. Hwang KS et al. 1987, The emissions of broadband electrostatic noise in the near vicinity of the shuttle orbiter, *Planet. Space Sci.*, **35**, 1373.
17. Papadopoulos KD 1984, On the shuttle glow (the plasma alternative), *Radio Science*, **19**, 571.
18. Cairns IH 1989, Electrostatic wave generation above and below the plasma frequency by electron beams, *Phys. Fluids B*, **1**, 204.
19. Musher SL et al. 1986, Nonlinear effects in the propagation of an ion beam across a magnetic field, *Sov. Phys. JETP*, **63**, 519.